


Up-down asymmetries and angular distributions in $D \rightarrow K_1(\rightarrow K\pi\pi)\ell^+\nu_\ell$

Lingzhu Bian¹, Liang Sun^{1,*} and Wei Wang^{2,†}

¹*School of Physics and Technology, Wuhan University, Wuhan 430072, China*

²*INPAC, Key Laboratory for Particle Astrophysics and Cosmology (MOE), Shanghai Key Laboratory for Particle Physics and Cosmology, School of Physics and Astronomy, Shanghai Jiao Tong University, Shanghai 200240, China*

 (Received 17 May 2021; accepted 12 July 2021; published 10 September 2021)

Using the helicity amplitude technique, we derive differential decay widths and angular distributions for the decay cascade $D \rightarrow K_1(1270, 1400)\ell^+\nu_\ell \rightarrow (K\pi\pi)\ell^+\nu_\ell$ ($\ell = e, \mu$), in which the electron and muon mass is explicitly included. Using a set of phenomenological results for $D \rightarrow K_1$ form factors, we calculate partial decay widths and branching fractions for $D^0 \rightarrow K_1^-\ell^+\nu_\ell$ and $D^+ \rightarrow K_1^0\ell^+\nu_\ell$, but find that results for $\mathcal{B}(D \rightarrow K_1(1270)e^+\nu_e)$ are about a factor 1.5 larger than recent BESIII measurements. We further demonstrate that the measurement of up-down asymmetry in $D \rightarrow K_1e^+\nu_e \rightarrow (K\pi\pi)e^+\nu_e$ and angular distributions in $D \rightarrow K_1\ell^+\nu_\ell \rightarrow (K\pi\pi)\ell^+\nu_\ell$ can help to determine the hadronic amplitude requested in $B \rightarrow K_1(\rightarrow K\pi\pi)\gamma$.

DOI: 10.1103/PhysRevD.104.053003

I. INTRODUCTION

Nowadays searching for new physics (NP) beyond the standard model (SM) is a most primary objective in particle physics. This can in principle proceed in two distinct directions. It is likely that new particles emerge directly in high energy collisions for instance at large hadron collider (LHC). On the other side, the NP particles can affect various low-energy observables by modifying the coupling strength or introducing new interaction forms and thus a high precision study of these observables is likely to indirectly access the NP. In the SM, the charged weak interaction has the $V - A$ chirality and thereby the photon in $b \rightarrow s\gamma$ is predominantly left-handed. The contribution with right-handed polarization is suppressed by the ratio of strange and bottom quark masses. Therefore the measurement of photon polarization in $b \rightarrow s\gamma$ provides a unique probe for new physics [1–3]. A representative scenario of this type is the left-right symmetric model [4,5], in which the photon can acquire a significant right-handed component.

In practice, the chirality of the $b \rightarrow s\gamma$ can be probed using the measurements of inclusive $B \rightarrow X_s\gamma$ decay branching fractions [6–9], the mixing-induced CP

asymmetries of radiative B^0 and B_s^0 decays [10–13] and the $B \rightarrow K^*e^+e^-$ with very low dilepton mass squared [14,15]. Interestingly, the photon helicity in radiative D decays was also explored [16,17].

In addition to the above methods, it is pointed out that the photon helicity in $b \rightarrow s\gamma$ is proportional to an up-down asymmetry \mathcal{A}_{UD} in $B \rightarrow K_1(\rightarrow K\pi\pi)\gamma$ [18–20] and more generally the angular distribution in $B \rightarrow K_{res}(\rightarrow K\pi\pi)\gamma$. Throughout this work we will use K_1 to denote the axial-vector meson $K_1(1270)$ and/or $K_1(1400)$. However the measurement of up-down asymmetry in $B \rightarrow K_1\gamma$ [21] was incapable to reveal the photon helicity due to the requirement of the detailed knowledge of K_1 decay dynamics. Many interesting theoretical analyses have adopted non-perturbative approaches to parametrize the $K_1 \rightarrow K\pi\pi$ decay amplitude and provided power constraints on the decay parameters [18–20,22,23]. In a previous work [24] it is proposed that one can tackle this problem by combining semileptonic $D \rightarrow K_1e^+\nu_e$ decays. In particular, a ratio of up-down asymmetries in $D \rightarrow K_1(\rightarrow K\pi\pi)e^+\nu_e$, \mathcal{A}'_{UD} , has been proposed to quantify the hadronic effects in $K_1 \rightarrow K\pi\pi$ decay. More explicitly the photon helicity can be expressed as a ratio of the two observables $\lambda_\gamma = 3/4 \times \mathcal{A}_{UD}/\mathcal{A}'_{UD}$ [24].

The purpose of this work is multifold. We will first provide the details in the helicity amplitude approach to derive the pertinent angular distributions and up-down asymmetries. Second, we will extend the previous analysis to the muon mode whose mass can not neglected in D decays. Using the phenomenological results for $D \rightarrow K_1$ form factors, we calculate partial decay widths for $D \rightarrow K_1\ell^+\nu_\ell$, and show that the measurement of up-down

* Corresponding author.
sunl@whu.edu.cn

† Corresponding author.
wei.wang@sjtu.edu.cn

Published by the American Physical Society under the terms of the [Creative Commons Attribution 4.0 International license](https://creativecommons.org/licenses/by/4.0/). Further distribution of this work must maintain attribution to the author(s) and the published article's title, journal citation, and DOI. Funded by SCOAP³.

asymmetry in $D \rightarrow K_1(\rightarrow K\pi\pi)e^+\nu_e$ and the angular distribution $D \rightarrow K_1(\rightarrow K\pi\pi)\mu^+\nu_\mu$ can help to determine the hadronic amplitude requested in $B \rightarrow K_1(\rightarrow K\pi\pi)\gamma$.

The rest of this paper is organized as follows. In Sec. II, we will give a detailed derivation of the angular distributions. In Sec. III, we will use the $D \rightarrow K_1$ form factors and calculate the differential decay widths. A comparison of predicted branching fractions with experimental data from BESIII measurements is made, and a MC simulation of angular distributions with the LHCb geometrical acceptance is also presented. The last section contains a brief summary.

II. FRAMEWORK AND ANGULAR DISTRIBUTIONS

In this section we will make use of the helicity amplitude technique and derive the angular distributions for the decay cascade $D \rightarrow K_1\ell^+\nu_\ell \rightarrow (K\pi\pi)\ell^+\nu_\ell$. Here the D and K_1 could be charged or neutral. Since a neutral π^0 is difficult to reconstruct especially at hadron colliders, it is more plausible to explore the $\pi^+\pi^-$. Thus in the following, we will consider the decay chain $D^0 \rightarrow K_1^-\ell^+\nu_\ell \rightarrow (K^-\pi^+\pi^-)\ell^+\nu_\ell$ and $D^+ \rightarrow \bar{K}_1^0\ell^+\nu_\ell \rightarrow (\bar{K}^0\pi^+\pi^-)\ell^+\nu_\ell$, though the results are also applicable to other decay channels with neutral pions. The kinematics of this decay cascade is shown in Fig. 1. In the lepton pair $\ell^+\nu_\ell$ rest frame, θ_ℓ is defined by the ℓ^+ flight direction and the opposite of the D meson flight direction. In K_1 rest frame, \vec{n} is defined as the normal direction of the decay plane, and θ_K is the relative angle between \vec{n} and the opposite of the D meson flight direction.

A few remarks on the kinematics are given in order.

- (i) The normal direction is not unambiguous. For instance, in K_1^- decay plane, it is likely to construct the normal direction with the momentum of π^+ and π^- , while the LHCb measurement of up-down asymmetry and angular distributions in $B \rightarrow K_1\gamma$ makes use of the slow and fast pion momenta [21], $\vec{n} \sim \vec{p}_{\pi,\text{slow}} \times \vec{p}_{\pi,\text{fast}}$.
- (ii) Second, since the \vec{n} is a cross product of two momenta, its direction will not be altered under parity transformation, but the flight direction of the D meson will be reversed. So the θ_K will be changed to $\pi - \theta_K$ under parity transformation, implying that the $\cos\theta_K$ is parity odd. The left-handed and right-handed polarization of K_1 gives opposite contributions to the $\cos\theta_K$ term.
- (iii) Third, weak interaction in $W^* \rightarrow \ell^+\nu_\ell$ violates parity conservation. Thus even though $\cos\theta_\ell$ is parity-even, the left-handed and right-handed contributions to the $\cos\theta_\ell$ term also differ in sign.
- (iv) Furthermore the definition of θ_K depends on charge or flavor of K_1 , namely the angle θ_K defined in K_1^- decay may differ with the one defined in K_1^+ system.

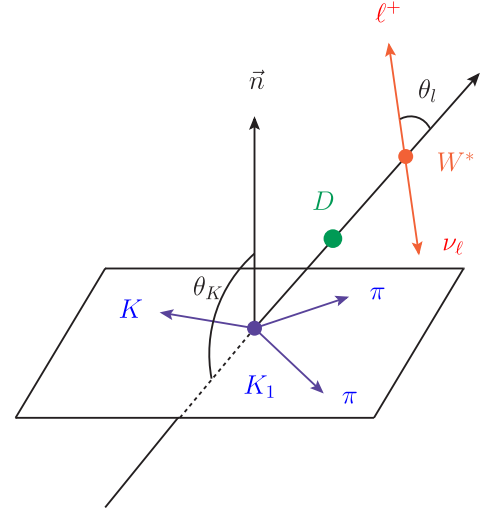


FIG. 1. The kinematics for $D \rightarrow K_1\ell^+\nu_\ell \rightarrow (K\pi\pi)\ell^+\nu_\ell$. In the lepton pair $\ell^+\nu_\ell$ rest frame, the angle θ_ℓ is defined by the ℓ^+ flight direction and the opposite of the D meson flight direction. In the K_1 rest frame the \vec{n} is defined as the normal direction of the K_1 decay plane, and θ_K is the relative angle between \vec{n} and the opposite of the D flight direction. Since \vec{n} is made of the cross product of two momenta, its direction will not be altered under parity transformation. But since the D flight direction will be reversed, the θ_K will be changed to $\pi - \theta_K$ under parity transformation, implying that the $\cos\theta_K$ is parity odd.

It is important to stick with the same convention on the kinematics in analyzing B and D decays.

Semileptonic decays of D into K_1 are induced by effective electro-weak Hamiltonian:

$$\mathcal{H} = \frac{G_F}{\sqrt{2}} V_{cs} \bar{s} \gamma^\mu (1 - \gamma_5) c \times \bar{\nu}_\ell \gamma_\mu (1 - \gamma_5) \ell, \quad (1)$$

where G_F is Fermi constant, and V_{cs} is CKM matrix element. With the above Hamiltonian, the partial decay width for semileptonic D decays can be generically written as

$$d\Gamma = \frac{(2\pi)^4}{2m_D} \times d\Phi_n \times \sum_{\text{spin}} |\mathcal{M}|^2. \quad (2)$$

Here $d\Phi_n$ denotes the n -body phase space. The pertinent decay amplitude \mathcal{M} can be decomposed into three individuals: $D \rightarrow K_1 W^*$, $K_1 \rightarrow K\pi\pi$ and $W^* \rightarrow \ell^+\nu_\ell$. Using the relation of $g_{\mu\nu}$ and polarization vector,

$$g_{\mu\nu} = - \sum_{\lambda=0,\pm 1} \epsilon_\mu^*(\lambda) \epsilon_\nu(\lambda) + \frac{q_\mu q_\nu}{q^2}, \quad (3)$$

one can disassemble decay amplitudes into a hadronic part and leptonic part

$$\mathcal{M} = \frac{G_F}{\sqrt{2}} V_{cs} H^\mu L^\nu g_{\mu\nu} = \frac{G_F}{\sqrt{2}} V_{cs} \left[-\sum_{\lambda} H \cdot \epsilon^*(\lambda) \times L \cdot \epsilon(\lambda) + H \cdot \epsilon^*(t) \times L \cdot \epsilon(t) \right], \quad (4)$$

with $\epsilon^\mu(t) \equiv q^\mu / \sqrt{q^2}$. After this decomposition, both hadronic and leptonic parts are Lorentz invariant and thus can be calculated in convenient reference frames. Actually the hadronic part could be further resolved into two individuals, namely $D \rightarrow K_1 W^*$ and $K_1 \rightarrow K \pi \pi$. Each individuals will be calculated in rest frame of the decaying particle.

A. The leptonic amplitude for $W^* \rightarrow \ell^+ \nu_\ell$

For simplicity, we introduce the abbreviation,

$$\begin{aligned} L(\lambda_e, \lambda_\nu, \lambda_W = 0, \pm 1) &= L^\mu \epsilon_\mu(\lambda) = \bar{u}_\nu \gamma^\mu (1 - \gamma_5) v_\ell \epsilon_\mu(\lambda), \\ L(\lambda_e, \lambda_\nu, \lambda_W = t) &= L^\mu \frac{q_\mu}{\sqrt{q^2}} = \bar{u}_\nu \gamma^\mu (1 - \gamma_5) v_\ell \frac{q_\mu}{\sqrt{q^2}}, \end{aligned} \quad (5)$$

where all spin/helicity indices are explicitly shown. Introducing $f_l = i\sqrt{2(q^2 - m_\ell^2)}$ and using $\hat{m}_\ell = m_\ell / \sqrt{q^2}$, one can obtain the nonvanishing leptonic decay amplitude:

$$\begin{aligned} L\left(\lambda_e = -\frac{1}{2}, \lambda_\nu = -\frac{1}{2}, \lambda_W = -1\right) &= f_l \hat{m}_\ell \sin \theta_\ell, & L\left(\lambda_e = -\frac{1}{2}, \lambda_\nu = -\frac{1}{2}, \lambda_W = 0\right) &= -f_l \sqrt{2} \hat{m}_\ell \cos \theta_\ell, \\ L\left(\lambda_e = -\frac{1}{2}, \lambda_\nu = -\frac{1}{2}, \lambda_W = 1\right) &= -f_l \hat{m}_\ell \sin \theta_\ell, & L\left(\lambda_e = -\frac{1}{2}, \lambda_\nu = -\frac{1}{2}, t\right) &= f_l \sqrt{2} \hat{m}_\ell \\ L\left(\lambda_e = \frac{1}{2}, \lambda_\nu = -\frac{1}{2}, \lambda_W = -1\right) &= -f_l (1 + \cos \theta_\ell), & L\left(\lambda_e = \frac{1}{2}, \lambda_\nu = -\frac{1}{2}, \lambda_W = 0\right) &= -f_l \sqrt{2} \sin \theta_\ell, \\ L\left(\lambda_e = \frac{1}{2}, \lambda_\nu = -\frac{1}{2}, \lambda_W = 1\right) &= -f_l (1 - \cos \theta_\ell). \end{aligned} \quad (6)$$

In the massless limit $m_\ell \rightarrow 0$, only the last three terms are nonzero due to the helicity conservation.

B. $D \rightarrow K_1 W^*$

The $D \rightarrow K_1$ transition matrix element can be parametrized by a set of form factors:

$$\langle K_1 | \bar{s} \gamma^\mu \gamma_5 c | D \rangle = -\frac{2iA(q^2)}{m_D - m_{K_1}} \epsilon^{\mu\nu\rho\sigma} (\epsilon_{K_1}^*)_\nu (p_D)_\rho (p_{K_1})_\sigma, \quad (7)$$

$$\begin{aligned} \langle K_1 | \bar{s} \gamma^\mu c | D \rangle &= -2m_{K_1} V_0(q^2) \frac{\epsilon_{K_1}^* \cdot q}{q^2} q^\mu - (m_D - m_{K_1}) V_1(q^2) \left[\epsilon_{K_1}^* - \frac{\epsilon_{K_1}^* \cdot q}{q^2} q^\mu \right] \\ &+ V_2(q^2) \frac{\epsilon_{K_1}^* \cdot q}{m_D - m_{K_1}} \left[(p_D + p_{K_1})^\mu - \frac{m_D^2 - m_{K_1}^2}{q^2} q^\mu \right], \end{aligned} \quad (8)$$

where $q^\mu = p_D^\mu - p_{K_1}^\mu$ is the momentum transfer and $\epsilon^{\mu\nu\rho\sigma}$ is the antisymmetric tensor. So the matrix element $c_{\lambda_W} \equiv \langle K_1 | \bar{s} \gamma^\mu (1 - \gamma_5) c | D \rangle \epsilon_\mu^*(\lambda_W)$ is evaluated as

$$c_{\pm} = (m_D - m_{K_1}) V_1 \mp \frac{A \sqrt{\lambda(m_D^2, m_{K_1}^2, q^2)}}{m_D - m_{K_1}}, \quad (9)$$

$$c_0 = \frac{-1}{2m_{K_1} \sqrt{q^2}} \left[(m_D^2 - m_{K_1}^2 - q^2) (m_D - m_{K_1}) V_1 - \frac{\lambda(m_D^2, m_{K_1}^2, q^2)}{m_D - m_{K_1}} V_2 \right], \quad (10)$$

$$c_t = -\frac{\sqrt{\lambda(m_D^2, m_{K_1}^2, q^2)}}{\sqrt{q^2}} V_0. \quad (11)$$

In the above, $\lambda(m_D^2, m_{K_1}^2, q^2) = (m_D^2 + m_{K_1}^2 - q^2)^2 - 4m_D^2 m_{K_1}^2$.

C. Differential decay width for $D \rightarrow K_1 \ell^+ \nu_\ell$

In this subsection, we will derive the differential decay width for $D \rightarrow K_1 \ell^+ \nu_\ell$. In the narrow width limit for K_1 , this decay width gives a normalization for the angular distributions for $D \rightarrow K_1 (\rightarrow K\pi\pi) \ell^+ \nu_\ell$.

Combining the three-body phase space

$$\begin{aligned} d\Phi_3(p_{K_1}, p_\ell, p_{\nu_\ell}) &= \delta^4(p_D - p_{K_1} - p_{\ell^+} - p_{\nu_\ell}) \frac{d^3 p_{K_1}}{(2\pi)^3 2E_{K_1}} \frac{d^3 p_{\ell^+}}{(2\pi)^3 2E_{\ell^+}} \frac{d^3 p_{\nu_\ell}}{(2\pi)^3 2E_{\nu_\ell}} \\ &= \delta^4(p_D - p_{K_1} - q)(2\pi)^4 \delta^4(q - p_{\ell^+} - p_{\nu_\ell}) \frac{d^4 q}{(2\pi)^4} \frac{d^3 p_{K_1}}{(2\pi)^3 2E_{K_1}} \frac{d^3 p_{\ell^+}}{(2\pi)^3 2E_{\ell^+}} \frac{d^3 p_{\nu_\ell}}{(2\pi)^3 2E_{\nu_\ell}} \\ &= \frac{1}{(2\pi)^7} \frac{\sqrt{\lambda(m_D^2, m_{K_1}^2, q^2)}}{32m_D^2} (1 - m_\ell^2/q^2) \times d\cos\theta_\ell dq^2, \end{aligned} \quad (12)$$

one can obtain the angular distribution for $D \rightarrow K_1 \ell^+ \nu_\ell$

$$\begin{aligned} \frac{d\Gamma}{dq^2 d\cos\theta_\ell} &= \frac{G_F^2 |V_{cs}|^2 \sqrt{\lambda(m_D^2, m_{K_1}^2, q^2)} q^2}{512\pi^3 m_D^3} (1 - \hat{m}_\ell^2)^2 \times (2c_0^2 (\sin^2\theta_\ell + \hat{m}_\ell^2 \cos^2\theta_\ell) \\ &\quad + c_+^2 [(1 + \cos\theta_\ell)^2 + \hat{m}_\ell^2 \sin^2\theta_\ell] + c_-^2 [(1 - \cos\theta_\ell)^2 + \hat{m}_\ell^2 \sin^2\theta_\ell] + c_t^2 2\hat{m}_t^2 - \text{Re}[c_0 c_t^*] 4\hat{m}_t^2 \cos\theta). \end{aligned} \quad (13)$$

Integrating over $\cos\theta_\ell$, one can have partial decay widths [25,26]:

$$\begin{aligned} \frac{d\Gamma_L(D \rightarrow K_1 \ell^+ \nu_\ell)}{dq^2} &= \frac{G_F^2 |V_{cs}|^2 \sqrt{\lambda(m_D^2, m_{K_1}^2, q^2)} q^2}{512\pi^3 m_D^3} (1 - \hat{m}_\ell^2)^2 \times \left(\frac{4}{3} c_0^2 (2 + \hat{m}_\ell^2) + 4\hat{m}_\ell^2 c_t^2 \right) \\ &= \frac{\sqrt{\lambda(m_D^2, m_{K_1}^2, q^2)} G_F^2 |V_{cs}|^2}{384m_D^3 \pi^3} (1 - \hat{m}_\ell^2)^2 \times \left\{ 3\hat{m}_t^2 \lambda(m_D^2, m_{K_1}^2, q^2) V_0^2 \right. \\ &\quad \left. + (\hat{m}_\ell^2 + 2) \left| \frac{1}{2m_{K_1}} \left[(m_D^2 - m_{K_1}^2 - q^2)(m_D - m_{K_1}) V_1 - \frac{\lambda(m_D^2, m_{K_1}^2, q^2)}{m_D - m_{K_1}} V_2 \right] \right|^2 \right\}, \end{aligned} \quad (14)$$

$$\begin{aligned} \frac{d\Gamma_\pm(D \rightarrow K_1 \ell^+ \nu_\ell)}{dq^2} &= \frac{G_F^2 |V_{cs}|^2 \sqrt{\lambda(m_D^2, m_{K_1}^2, q^2)} q^2}{512\pi^3 m_D^3} (1 - \hat{m}_\ell^2)^2 \times \frac{4}{3} c_\pm^2 (2 + \hat{m}_\ell^2) \\ &= \frac{\sqrt{\lambda(m_D^2, m_{K_1}^2, q^2)} G_F^2 |V_{cs}|^2}{384m_D^3 \pi^3} (1 - \hat{m}_\ell^2)^2 q^2 \\ &\quad \times \left\{ (\hat{m}_\ell^2 + 2) \lambda(m_D^2, m_{K_1}^2, q^2) \left| \frac{A}{m_D - m_{K_1}} \mp \frac{(m_D - m_{K_1}) V_1}{\sqrt{\lambda(m_D^2, m_{K_1}^2, q^2)}} \right|^2 \right\}, \end{aligned} \quad (15)$$

where L and \pm in the subscripts denote contribution from longitudinal and transverse polarization.

D. $K_1 \rightarrow K\pi\pi$

The hadronic part in the decay cascade $D \rightarrow K_1 \ell^+ \nu_\ell \rightarrow (K\pi\pi) \ell^+ \nu_\ell$ contains:

$$H \cdot \epsilon_W^*(\lambda) \sim \langle K\pi\pi | K_1 \rangle \times \langle K_1 | (V - A)_\mu | D \rangle \epsilon_W^{*\mu}(\lambda), \quad (16)$$

where $\langle K\pi\pi | K_1 \rangle$ is parameterized as

$$\langle K\pi\pi | K_1 \rangle = (2\pi)^4 \delta^4(p_{K_1} - p_K - p_\pi - p_\pi) \times \epsilon_{K_1} \cdot J. \quad (17)$$

Notice that the explicit form of J depends on the convention of the \vec{n} .

In the K_1 rest frame, one can set the normal direction as the z -axis and the momenta of (K, π^+, π^-) lies in the x - y plane. Since J is a linear combination of the momenta of two pions, $J_z = 0$ and

$$J_\mu = (J_0, J_x, J_y, 0). \quad (18)$$

To simplify the calculation, we choose K_1 moving along (θ_K, ϕ) direction, and thus $\epsilon_{K_1} \cdot J$ is evaluated as

$$\epsilon_{K_1}(0) \cdot J = \sin \theta_K (J_x \cos \phi + J_y \sin \phi), \quad (19)$$

$$\epsilon_{K_1}(1) \cdot J = -\frac{1}{\sqrt{2}} [\cos \phi (J_x \cos \theta_K + iJ_y) + \sin \phi (J_y \cos \theta_K - iJ_x)], \quad (20)$$

$$\epsilon_{K_1}(-1) \cdot J = \frac{1}{\sqrt{2}} [\cos \phi (J_x \cos \theta_K - iJ_y) + \sin \phi (J_y \cos \theta_K + iJ_x)]. \quad (21)$$

E. Angular distributions in $D \rightarrow K_1 \ell^+ \nu_\ell \rightarrow (K\pi\pi) \ell^+ \nu_\ell$

With the above individuals, one can obtain the total decay amplitude:

$$\begin{aligned} \mathcal{M}\left(\lambda_\ell = -\frac{1}{2}\right) &= L\left(\lambda_e = -\frac{1}{2}, \lambda_\nu = -\frac{1}{2}, \lambda_W = -1\right) \times \epsilon_{K_1}(-1) \cdot J \times c_- \\ &\quad + L\left(\lambda_\ell = -\frac{1}{2}, \lambda_\nu = -\frac{1}{2}, \lambda_W = 1\right) \times \epsilon_{K_1}(1) \cdot J \times c_+ \\ &\quad + L\left(\lambda_\ell = -\frac{1}{2}, \lambda_\nu = -\frac{1}{2}, \lambda_W = 0\right) \times \epsilon_{K_1}(0) \cdot J \times c_0 \\ &\quad - L\left(\lambda_\ell = -\frac{1}{2}, \lambda_\nu = -\frac{1}{2}, \lambda_W = t\right) \times \epsilon_{K_1}(0) \cdot J \times c_t, \end{aligned} \quad (22)$$

$$\begin{aligned} \mathcal{M}\left(\lambda_\ell = \frac{1}{2}\right) &= L\left(\lambda_e = \frac{1}{2}, \lambda_\nu = -\frac{1}{2}, \lambda_W = -1\right) \times \epsilon_{K_1}(-1) \cdot J \times c_- \\ &\quad + L\left(\lambda_\ell = \frac{1}{2}, \lambda_\nu = -\frac{1}{2}, \lambda_W = 1\right) \times \epsilon_{K_1}(1) \cdot J \times c_+ \\ &\quad + L\left(\lambda_\ell = \frac{1}{2}, \lambda_\nu = -\frac{1}{2}, \lambda_W = 0\right) \times \epsilon_{K_1}(0) \cdot J \times c_0 \\ &\quad - L\left(\lambda_e = \frac{1}{2}, \lambda_\nu = -\frac{1}{2}, \lambda_W = t\right) \times \epsilon_{K_1}(0) \cdot J \times c_t. \end{aligned} \quad (23)$$

Using two abbreviations:

$$|J|^2 = |J_x|^2 + |J_y|^2, \quad \text{Im}[n \cdot (\vec{J} \times \vec{J}^*)] = -i(J_x J_y^* - J_y J_x^*), \quad (24)$$

and integrating over ϕ , we obtain:

$$\begin{aligned}
|\mathcal{M}|^2 &= \frac{3}{4\pi|J|^2} \int d\phi \left(\left| \mathcal{M} \left(\lambda_e = \frac{1}{2} \right) \right|^2 + \left| \mathcal{M} \left(\lambda_e = -\frac{1}{2} \right) \right|^2 \right) \\
&= \frac{3}{8} (d_1 + d'_1 [\cos^2 \theta_K \cos^2 \theta_\ell] + d_2 \cos \theta_\ell + d'_2 \cos^2 \theta_K \cos \theta_\ell \\
&\quad + d_3 \cos \theta_K + d'_3 \cos \theta_K \cos^2 \theta_\ell + d_4 \cos \theta_K \cos \theta_\ell + d_5 \cos^2 \theta_K + d'_5 \cos^2 \theta_\ell), \tag{25}
\end{aligned}$$

where a factor $\frac{3}{4\pi|J|^2}$ is introduced to be consistent with the three-body decay width. In the above equation, the angular coefficients are calculated as

$$\begin{aligned}
d_1 &= (1 + \hat{m}_\ell^2)(|c_-|^2 + |c_+|^2) + 4|c_0|^2 + 4\hat{m}_\ell^2|c_t|^2, \\
d'_1 &= (1 - \hat{m}_\ell^2)(4|c_0|^2 + |c_-|^2 + |c_+|^2), \\
d_2 &= -2[|c_-|^2 - |c_+|^2 + 4\text{Re}[c_0 c_t^*] \hat{m}_\ell^2], \\
d'_2 &= -2[|c_-|^2 - |c_+|^2 - 4\text{Re}[c_0 c_t^*] \hat{m}_\ell^2], \\
d_3 &= 2 \frac{\text{Im}[\vec{n} \cdot (\vec{J} \times \vec{J}^*)]}{|J|^2} [(1 + \hat{m}_\ell^2)(|c_+|^2 - |c_-|^2)], \\
d'_3 &= 2 \frac{\text{Im}[\vec{n} \cdot (\vec{J} \times \vec{J}^*)]}{|J|^2} [(1 - \hat{m}_\ell^2)(|c_+|^2 - |c_-|^2)] \\
d_4 &= 4 \frac{\text{Im}[\vec{n} \cdot (\vec{J} \times \vec{J}^*)]}{|J|^2} (|c_-|^2 + |c_+|^2), \\
d_5 &= -[(1 + \hat{m}_\ell^2)(-|c_-|^2 - |c_+|^2) + 4|c_0|^2 + 4\hat{m}_\ell^2|c_t|^2], \\
d'_5 &= -[(1 - \hat{m}_\ell^2)(4|c_0|^2 - |c_-|^2 - |c_+|^2)]. \tag{26}
\end{aligned}$$

Apparently the following combination can be used to extract the hadron amplitude H_{K_1}

$$H_{K_1} = \frac{d_3 + d'_3}{d_2 + d'_2} = \frac{\text{Im}[\vec{n} \cdot (\vec{J} \times \vec{J}^*)]}{|J|^2}. \tag{27}$$

Including the phase-space, we arrive at the angular distribution for $D \rightarrow K_1 \ell^+ \nu_\ell \rightarrow K \pi \pi \ell^+ \nu_\ell$ as:

$$\begin{aligned}
\frac{d\Gamma}{dq^2 d\cos\theta_\ell d\cos\theta_K} &= \frac{G_F^2 |V_{cs}|^2 q^2 \sqrt{\lambda(m_D^2, m_{K_1}^2, q^2)}}{512\pi^3 m_D^3} (1 - \hat{m}_\ell^2)^2 \times \frac{3}{8} (d_1 + d'_1 [\cos^2 \theta_K \cos^2 \theta_\ell] + d_2 \cos \theta_\ell + d'_2 \cos^2 \theta_K \cos \theta_\ell \\
&\quad + d_3 \cos \theta_K + d'_3 \cos \theta_K \cos^2 \theta_\ell + d_4 \cos \theta_K \cos \theta_\ell + d_5 \cos^2 \theta_K + d'_5 \cos^2 \theta_\ell). \tag{28}
\end{aligned}$$

The ratio of differential up-down asymmetries [24] is evaluated as:

$$\begin{aligned}
\mathcal{A}'_{\text{UD}} &\equiv \frac{\frac{d\Gamma}{dq^2} [\cos \theta_K > 0] - \frac{d\Gamma}{dq^2} [\cos \theta_K < 0]}{\frac{d\Gamma}{dq^2} [\cos \theta_\ell > 0] - \frac{d\Gamma}{dq^2} [\cos \theta_\ell < 0]} \\
&= \frac{3d_3 + d'_3}{3d_2 + d'_2} \\
&= H_{K_1} \frac{(2 + \hat{m}_\ell^2)(|c_-|^2 - |c_+|^2)}{2[|c_-|^2 - |c_+|^2] + 2\text{Re}[c_0 c_t^*] \hat{m}_\ell^2}. \tag{29}
\end{aligned}$$

If the massless limit $\hat{m}_\ell \rightarrow 0$, the above ratio is reduced to the hadronic amplitude H_{K_1} , but apparently this reduction is contaminated by the lepton mass.

F. Angular distributions in $B \rightarrow K_1\gamma$

In this subsection, we will derive the angular distribution in $B \rightarrow K_1(\rightarrow K\pi\pi)\gamma$. The effective Hamiltonian for $b \rightarrow s\gamma$ has the general form:

$$\mathcal{H}_{\text{eff}} = -\frac{4G_F}{\sqrt{2}}V_{tb}V_{ts}^*(C_{7L}\mathcal{O}_{7L} + C_{7R}\mathcal{O}_{7R}),$$

$$\mathcal{O}_{7L,R} = \frac{em_b}{16\pi^2}\bar{s}\sigma_{\mu\nu}\frac{1 \pm \gamma_5}{2}bF^{\mu\nu}, \quad (30)$$

where $C_{7L,7R}$ are the corresponding Wilson coefficients for $\mathcal{O}_{7L,R}$. Due to the chirality structure of W^\pm in SM, the photon in $b \rightarrow s\gamma$ is predominantly left-handed, while the right-handed polarization is suppressed by approximately m_s/m_b .

Using the helicity amplitude technique one can similarly calculate the angular distributions for $B \rightarrow K_1(\rightarrow K\pi\pi)\gamma$, and the results are easier in two aspects. First, there is no leptonic part in the decay cascade. Second, the $B \rightarrow K_1\gamma$ decay amplitudes only contain two polarizations. Without including higher order QCD corrections, the two polarization contributions are proportionally to $C_{7L,7R}$. Then differential decay rate for $B \rightarrow K_1(\rightarrow K\pi\pi)\gamma$ can be expressed as [18,19,23]:

$$\frac{d\Gamma_{K_1\gamma}}{d\cos\theta_K} = \frac{|A|^2|\vec{J}|^2}{4} \times \left[1 + \cos^2\theta_K + 2\lambda_\gamma \cos\theta_K \frac{\text{Im}[\vec{n} \cdot (\vec{J} \times \vec{J}^*)]}{|\vec{J}|^2} \right]. \quad (31)$$

Here the θ_K is the same angle as in Fig. 1. The non-perturbative amplitude A characterizes the $B \rightarrow K_1\gamma$. The photon polarization λ_γ is defined as

$$\lambda_\gamma \equiv \frac{|\mathcal{A}(B \rightarrow K_{1R}\gamma_R)|^2 - |\mathcal{A}(B \rightarrow K_{1L}\gamma_L)|^2}{|\mathcal{A}(B \rightarrow K_{1R}\gamma_R)|^2 + |\mathcal{A}(B \rightarrow K_{1L}\gamma_L)|^2}, \quad (32)$$

with $\lambda_\gamma \simeq -1$ for $b \rightarrow s\gamma$ but $\lambda_\gamma \simeq +1$ for $\bar{b} \rightarrow \bar{s}\gamma$ in SM.

III. NUMERICAL RESULTS AND DISCUSSIONS

A. K_1 mixing and $D \rightarrow K_1$ form factors

If the quark model is employed, two kinds of axial-vector states with a strange quark can be constructed, depending on the spin of the quark and anti-quark pair. If their total spin is 1, the resulting axial-vector state is denoted as 3P_1 , also called K_{1A} . When the total spin is 0, the axial-vector state is usually denoted as 1P_1 or K_{1B} . Since strange quark is heavier than up/down quark, $K_1(1270)$ and $K_1(1400)$ are not purely $K_{1A}({}^3P_1)$ and $K_{1B}({}^1P_1)$ states, and instead they will mix:

$$|K_1(1270)\rangle = |K_{1A}\rangle \sin\Theta_K + |K_{1B}\rangle \cos\Theta_K, \quad (33)$$

$$|K_1(1400)\rangle = |K_{1A}\rangle \cos\Theta_K - |K_{1B}\rangle \sin\Theta_K. \quad (34)$$

Generally, the mixing angle Θ_K can be determined by the experimental data, such as $\tau^- \rightarrow K_1^-\nu_\tau$, whose decay rate is given by

$$\Gamma(\tau^- \rightarrow K_1^-\nu_\tau) = \frac{m_\tau^3}{16\pi}G_F^2|V_{us}|^2f_A^2\left(1 - \frac{m_A^2}{m_\tau^2}\right)^2\left(1 + \frac{2m_A^2}{m_\tau^2}\right). \quad (35)$$

The measured branching fractions [27] are given as

$$\mathcal{B}(\tau^- \rightarrow K_1(1270)\nu_\tau) = (4.7 \pm 1.1) \times 10^{-3}, \quad (36)$$

$$\mathcal{B}(\tau^- \rightarrow K_1(1400)\nu_\tau) = (1.7 \pm 2.6) \times 10^{-3}, \quad (37)$$

through which one can extract the decay constants of K_1 :

$$|f_{K_1(1270)}| = (169_{-21}^{+19}) \text{ MeV};$$

$$|f_{K_1(1400)}| = (125_{-125}^{+74}) \text{ MeV}. \quad (38)$$

One can combine the decay constants for K_{1A} , K_{1B} evaluated for instance in QCD sum rules [28] to determine the mixing angle Θ_K [25]:

$$-143^\circ < \Theta_K < -120^\circ, \quad \text{or}$$

$$-49^\circ < \Theta_K < -27^\circ, \quad \text{or}$$

$$37^\circ < \Theta_K < 60^\circ, \quad \text{or}$$

$$131^\circ < \Theta_K < 153^\circ. \quad (39)$$

The mixing angle can be further constrained with the data on, such as $B \rightarrow K_1\gamma$ decays, and it is found that except the third scenario, the other three scenarios are not favored by K_1 masses or $B \rightarrow K_1\gamma$ decay widths [29]. With the available constraints, Ref. [30] suggested the use of $\Theta_K = 50.8^\circ$, while $\Theta_K = 33^\circ$ is suggested in Ref. [31]. In the following we will use $\Theta_K = 45^\circ$ as the central result [which is also favored by BESIII measurements of $\mathcal{B}(D \rightarrow K_1e^+\nu_e)$], but the dependence on Θ_K in a wider range $30^\circ < \Theta_K < 60^\circ$ will be presented. However it should be noticed that this range is obtained in conjunction with the form factors calculated in the covariant light-front quark model (LFQM) [30–33]. The $D \rightarrow K_1$ form factors have also been calculated in QCD sum rules [34–36], but results differ significantly. The corresponding mixing angle is obtained differently: $\Theta_K = -(34 \pm 13)^\circ$, which we shall adopt for consistence in the following comparison.

The results for $D \rightarrow K_1$ form factors from Refs. [30,33,34] are collected in Table I. In these results, the q^2 -distribution of form factors is parametrized as:

TABLE I. The $D \rightarrow K_1$ form factors calculated in the covariant LFQM [30,33] and QCD sum rules [34]. The coefficients a and b are parameters in Eq. (40) and (41). The physical K_1 states ($K_1(1270)$ and $K_1(1420)$) are mixtures of the K_{1A} ($J^{PC} = 1^{++}$) and K_{1B} ($J^{PC} = 1^{+-}$).

F [33]	$F(0)$	a	b	F	$F(0)$	a	b
$A^{DK_{1A}}$	0.98	0.92	0.17	$V_0^{DK_{1A}}$	0.34	1.44	0.15
$V_1^{DK_{1A}}$	2.02	-0.01	0.03	$V_2^{DK_{1A}}$	0.03	-0.18	0.10
$A^{DK_{1B}}$	0.10	1.03	0.48	$V_0^{DK_{1B}}$	0.44	0.80	0.27
$V_1^{DK_{1B}}$	1.53	0.39	0.05	$V_2^{DK_{1B}}$	-0.09	-0.16	0.51
F [30]	$F(0)$	a	b	F	$F(0)$	a	b
$A^{DK_{1A}}$	$0.15_{-0.01-0.01}^{+0.01+0.01}$	$0.89_{-0.03-0.01}^{+0.03+0.00}$	$0.12_{-0.02-0.01}^{+0.02+0.01}$	$V_0^{DK_{1A}}$	$0.28_{-0.00-0.00}^{+0.00+0.00}$	$0.84_{-0.02-0.01}^{+0.01-0.01}$	$0.39_{-0.05-0.03}^{+0.06+0.04}$
$V_1^{DK_{1A}}$	$1.60_{-0.05-0.02}^{+0.05+0.01}$	$-0.22_{-0.00-0.03}^{+0.00+0.03}$	$0.07_{-0.00+0.00}^{+0.00-0.00}$	$V_2^{DK_{1A}}$	$0.01_{-0.00+0.00}^{+0.00-0.00}$	$-0.83_{-0.17+0.02}^{+0.15-0.03}$	$0.24_{-0.03+0.01}^{+0.04-0.01}$
$A^{DK_{1B}}$	$0.10_{-0.00-0.00}^{+0.00+0.00}$	$0.98_{-0.01-0.01}^{+0.01+0.01}$	$0.37_{-0.03-0.03}^{+0.03+0.04}$	$V_0^{DK_{1B}}$	$0.48_{-0.01+0.02}^{+0.01-0.03}$	$0.94_{-0.02-0.02}^{+0.01+0.01}$	$0.22_{-0.00+0.03}^{+0.00-0.03}$
$V_1^{DK_{1B}}$	$1.58_{-0.02+0.03}^{+0.02+0.03}$	$0.31_{-0.02-0.01}^{+0.02+0.02}$	$0.04_{-0.00-0.00}^{+0.00+0.01}$	$V_2^{DK_{1B}}$	$-0.13_{-0.01+0.01}^{+0.01-0.01}$	$0.57_{-0.06-0.01}^{+0.04-0.01}$	$0.32_{-0.03+0.06}^{+0.05-0.04}$
F [34]	$F(0)$	a	b	F	$F(0)$	a	b
$A^{DK_{1A}}$	0.07	0.21	-2.14	$V_0^{DK_{1A}}$	0.11	0.44	0.61
$V_1^{DK_{1A}}$	0.37	0.20	-0.13	$V_2^{DK_{1A}}$	-0.03	-0.70	1.81
$A^{DK_{1B}}$	-0.53	0.46	0.38	$V_0^{DK_{1B}}$	-0.42	-2.33	9.24
$V_1^{DK_{1B}}$	-0.29	1.17	1.72	$V_2^{DK_{1B}}$	0.31	-0.49	-0.21

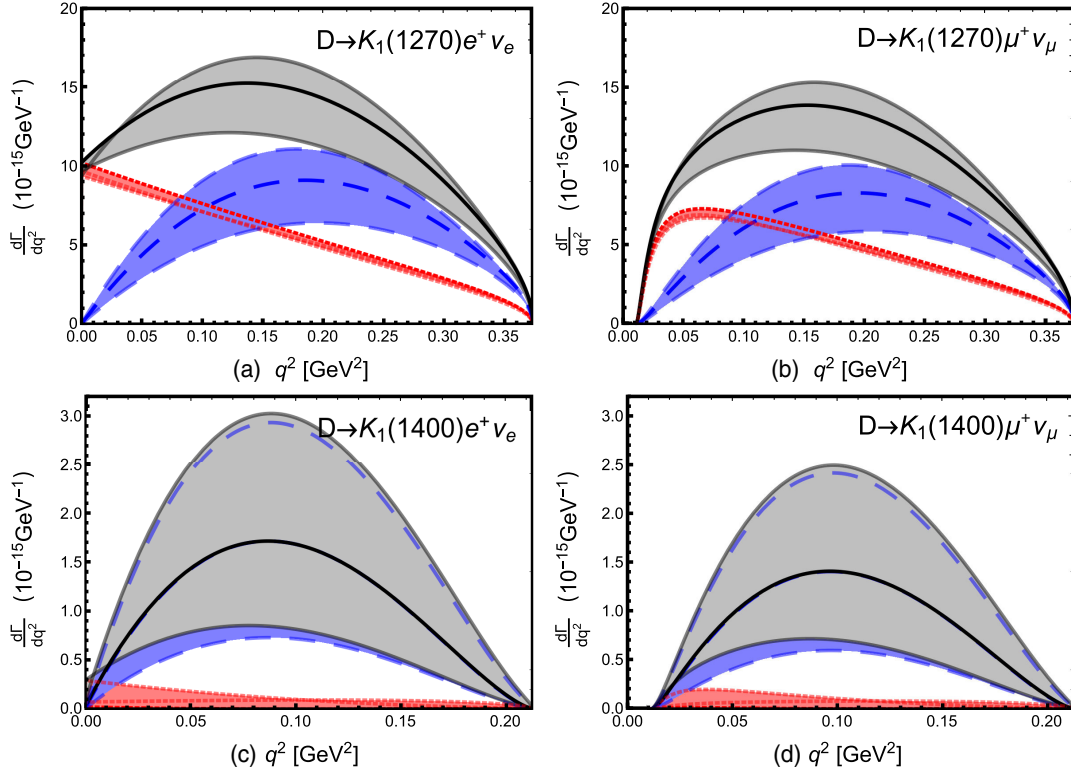


FIG. 2. Differential decay widths for $D \rightarrow K_1(1270)\ell^+\nu_\ell$ (in units of $10^{-15} \text{ GeV}^{-1}$) and $D \rightarrow K_1(1400)\ell^+\nu_\ell$ (in units of $10^{-15} \text{ GeV}^{-1}$) based on the form factors from Ref. [33]. The dotted and dashed lines correspond to the longitudinal and transverse polarizations, while the solid line gives the total differential decay widths. The shadowed region arises from the uncertainties in the mixing angle θ_K .

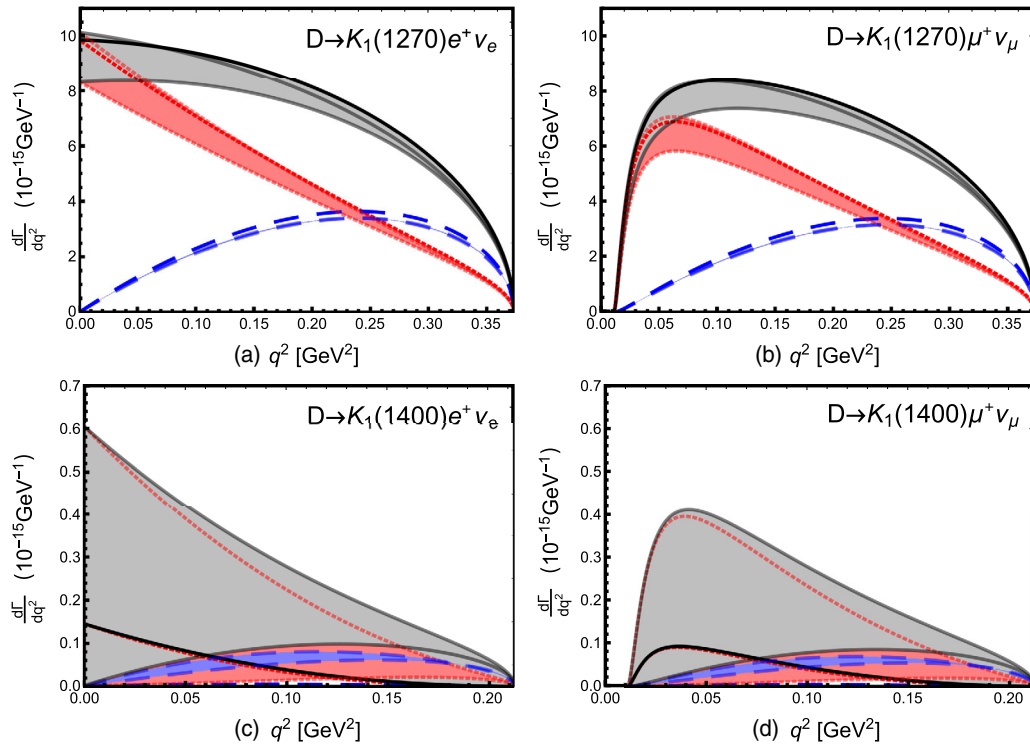


FIG. 3. Differential decay widths for $D \rightarrow K_1(1270)\ell^+\nu_\ell$ (in units of $10^{-15} \text{ GeV}^{-1}$) and $D \rightarrow K_1(1400)\ell^+\nu_\ell$ (in units of $10^{-15} \text{ GeV}^{-1}$) based on the form factors from Ref. [30]. The dotted and dashed lines correspond to the longitudinal and transverse polarizations, while the solid line gives the total differential decay widths. The shadowed region arises from the uncertainties in the mixing angle θ_K .

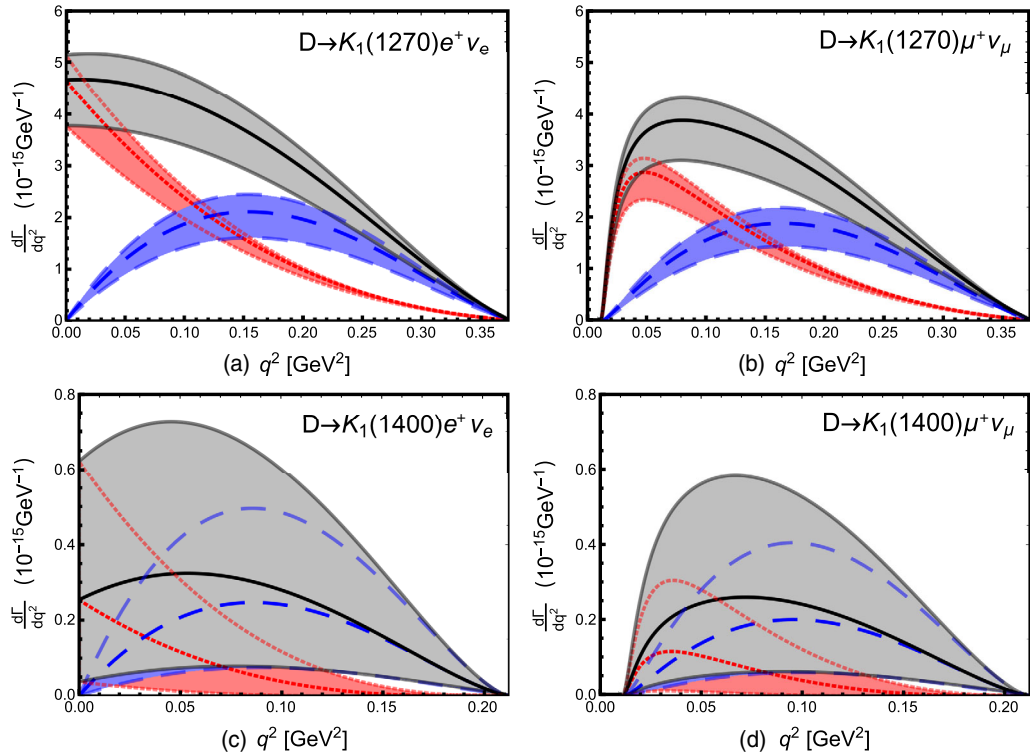


FIG. 4. Differential decay widths for $D \rightarrow K_1(1270)\ell^+\nu_\ell$ (in units of $10^{-15} \text{ GeV}^{-1}$) and $D \rightarrow K_1(1400)\ell^+\nu_\ell$ (in units of $10^{-15} \text{ GeV}^{-1}$), based on the form factors from QCD sum rules [34]. The dotted and dashed lines correspond to the longitudinal and transverse polarizations, while the solid line gives the total differential decay widths. The shadowed region arises from the uncertainties in the mixing angle θ_K .

$$F(q^2) = \frac{F(0)}{1 - aq^2/m_D^2 + b(q^2/m_D^2)^2}, \quad (40)$$

but a different parametrization is used for $V_2^{D \rightarrow K_{1B}}$ in Refs. [30,33]:

$$F(q^2) = \frac{F(0)}{(1 - q^2/m_D^2)(1 - aq^2/m_D^2 + b(q^2/m_D^2)^2)}. \quad (41)$$

The physical form factors are obtained through:

$$F^{D \rightarrow K_1(1270)} = F^{D \rightarrow K_{1A}} \sin \Theta_K + F^{D \rightarrow K_{1B}} \cos \Theta_K, \quad (42)$$

$$F^{D \rightarrow K_1(1400)} = F^{D \rightarrow K_{1A}} \cos \Theta_K - F^{D \rightarrow K_{1B}} \sin \Theta_K. \quad (43)$$

B. Decay widths and branching fractions

To calculate decay widths, we will use the following inputs from Particle Data Group [27]:

TABLE II. Results for integrated branching ratios for the $D \rightarrow K_1(1270)\ell^+\nu_\ell$ and $D \rightarrow K_1(1400)\ell^+\nu_\ell$ decays (in units of 10^{-3}). The experimental results are taken from BESIII measurements [37,38]. For each decay channel, three sets of theoretical predictions are given, which correspond to the form factors from Ref. [33], Ref. [30], and Ref. [34], respectively. Uncertainties from the mixing angle θ_K are also taken into account.

$D^0 \rightarrow K^-(1270)\ell^+\nu_\ell$	\mathcal{B}_L	\mathcal{B}_T	F_L	$\mathcal{B}_{\text{total}}$	$\mathcal{B}_{\text{data}}$
$\ell = e$	$1.3_{-0.094}^{+0}$	$1.5_{-0.42}^{+0.29}$	$0.47_{-0.06}^{+0.065}$	$2.7_{-0.51}^{+0.21}$	$1.09 \pm 0.13_{-0.16}^{+0.09} \pm 0.12$
	$1.2_{-0.16}^{+0.0058}$	$0.59_{-0.041}^{+0}$	$0.66_{-0.018}^{+0.017}$	$1.8_{-0.2}^{+0}$	
	$0.35_{-0.059}^{+0.026}$	$0.31_{-0.071}^{+0.047}$	$0.53_{-0.018}^{+0.02}$	$0.66_{-0.13}^{+0.074}$	
$\ell = \mu$	$1_{-0.075}^{+0}$	$1.3_{-0.36}^{+0.25}$	$0.45_{-0.059}^{+0.064}$	$2.3_{-0.44}^{+0.19}$...
	$0.94_{-0.13}^{+0.0058}$	$0.53_{-0.036}^{+0}$	$0.64_{-0.019}^{+0.018}$	$1.5_{-0.16}^{+0}$	
	$0.27_{-0.045}^{+0.019}$	$0.26_{-0.061}^{+0.04}$	$0.51_{-0.018}^{+0.02}$	$0.54_{-0.11}^{+0.06}$	
$D^+ \rightarrow \bar{K}^0(1270)\ell^+\nu_\ell$	\mathcal{B}_L	\mathcal{B}_T	F_L	$\mathcal{B}_{\text{total}}$	$\mathcal{B}_{\text{data}}$
$\ell = e$	$3.3_{-0.24}^{+0}$	$3.7_{-1.1}^{+0.74}$	$0.47_{-0.06}^{+0.065}$	$7_{-1.3}^{+0.54}$	$2.30 \pm 0.26_{-0.21}^{+0.18} \pm 0.25$
	$3_{-0.4}^{+0.015}$	$1.5_{-0.1}^{+0}$	$0.66_{-0.018}^{+0.017}$	$4.5_{-0.5}^{+0}$	
	$0.9_{-0.15}^{+0.066}$	$0.78_{-0.18}^{+0.12}$	$0.53_{-0.018}^{+0.02}$	$1.7_{-0.33}^{+0.19}$	
$\ell = \mu$	$2.6_{-0.19}^{+0}$	$3.2_{-0.92}^{+0.63}$	$0.45_{-0.059}^{+0.064}$	$5.9_{-1.1}^{+0.47}$...
	$2.4_{-0.33}^{+0.015}$	$1.3_{-0.092}^{+0}$	$0.64_{-0.019}^{+0.018}$	$3.7_{-0.41}^{+0}$	
	$0.69_{-0.11}^{+0.049}$	$0.67_{-0.15}^{+0.1}$	$0.51_{-0.018}^{+0.02}$	$1.4_{-0.27}^{+0.15}$	
$D^0 \rightarrow K^-(1400)\ell^+\nu_\ell$	\mathcal{B}_L	\mathcal{B}_T	F_L	$\mathcal{B}_{\text{total}}$	
$\ell = e$	$0.00056_0^{+0.014}$	$0.14_{-0.08}^{+0.1}$	$0.004_0^{+0.19}$	$0.14_{-0.067}^{+0.11}$...
	$0.0057_{-0.004}^{+0.026}$	$0.00044_0^{+0.0071}$	$0.93_{-0.74}^{+0}$	$0.0062_0^{+0.031}$	
	$0.0083_{-0.0074}^{+0.014}$	$0.02_{-0.014}^{+0.02}$	$0.29_{-0.16}^{+0.064}$	$0.028_{-0.021}^{+0.034}$	
$\ell = \mu$	$0.00066_0^{+0.011}$	$0.11_{-0.061}^{+0.079}$	$0.0062_0^{+0.2}$	$0.11_{-0.05}^{+0.087}$...
	$0.0046_{-0.0031}^{+0.02}$	$0.00034_0^{+0.0057}$	$0.93_{-0.74}^{+0}$	$0.0049_0^{+0.024}$	
	$0.0052_{-0.0047}^{+0.0094}$	$0.015_{-0.01}^{+0.015}$	$0.25_{-0.16}^{+0.068}$	$0.021_{-0.015}^{+0.025}$	
$D^+ \rightarrow \bar{K}^0(1400)\ell^+\nu_\ell$	\mathcal{B}_L	\mathcal{B}_T	F_L	$\mathcal{B}_{\text{total}}$	
$\ell = e$	$0.0014_0^{+0.035}$	$0.36_{-0.2}^{+0.26}$	$0.004_0^{+0.19}$	$0.36_{-0.17}^{+0.29}$...
	$0.015_{-0.01}^{+0.065}$	$0.0011_0^{+0.018}$	$0.93_{-0.74}^{+0}$	$0.016_0^{+0.078}$	
	$0.021_{-0.019}^{+0.035}$	$0.051_{-0.035}^{+0.051}$	$0.29_{-0.16}^{+0.064}$	$0.072_{-0.054}^{+0.087}$	
$\ell = \mu$	$0.0017_0^{+0.028}$	$0.27_{-0.15}^{+0.2}$	$0.0062_0^{+0.2}$	$0.27_{-0.13}^{+0.22}$...
	$0.012_{-0.0079}^{+0.05}$	$0.0008_0^{+0.014}$	$0.93_{-0.74}^{+0}$	$0.012_0^{+0.061}$	
	$0.013_{-0.012}^{+0.024}$	$0.039_{-0.026}^{+0.039}$	$0.25_{-0.16}^{+0.068}$	$0.052_{-0.038}^{+0.062}$	

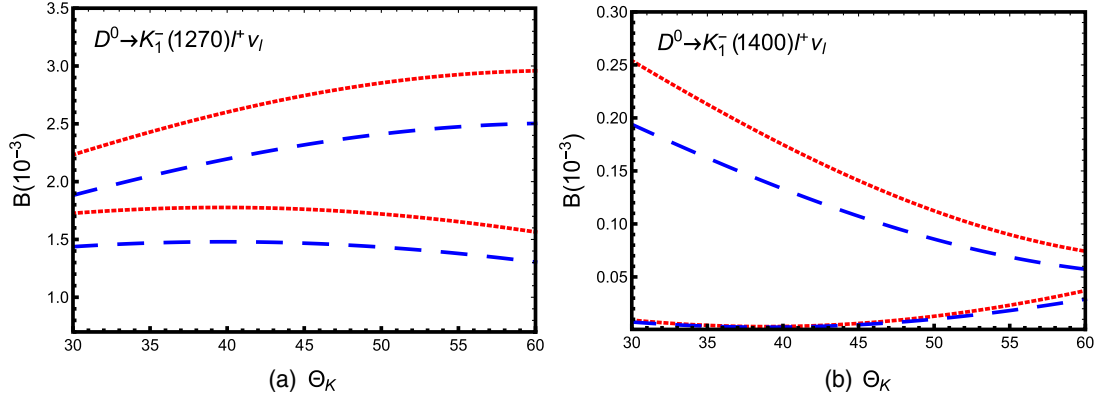


FIG. 5. Dependence of branching ratios $\mathcal{B}(D^0 \rightarrow K_1^- \ell^+ \nu_\ell)$ (in units of 10^{-3}) on the mixing angle Θ_K in the range $30^\circ < \Theta_K < 60^\circ$ based on the form factors from LFQM in Ref. [33] (the two upper lines), and Ref. [30] (the two lower curves). Dotted and dashed curves correspond to the electron and muon mode, respectively.

$$\tau(D^0) = (0.4101 \pm 0.0015) \times 10^{-12} \text{ s},$$

$$\tau(D^+) = (1.040 \pm 0.007) \times 10^{-12} \text{ s},$$

$$m_{K_1(1270)} = 1.253 \text{ GeV},$$

$$m_{K_1(1400)} = 1.403 \text{ GeV}, \quad V_{cs} = 0.973. \quad (44)$$

Differential decay widths $d\Gamma/dq^2$ (in units of $10^{-15} \text{ GeV}^{-1}$) for $D \rightarrow K_1(1270)\ell^+\nu_\ell$ and $D \rightarrow K_1(1400)\ell^+\nu_\ell$ are shown in Fig. 2, Fig. 3, and Fig. 4, respectively. The dotted and dashed lines correspond to the longitudinal and transverse polarizations, while the solid line gives the total differential decay widths. The shadowed region arises from the uncertainties in the mixing angle θ_K .

Results for integrated branching ratios for the $D \rightarrow K_1(1270)\ell^+\nu_\ell$ and $D \rightarrow K_1(1400)\ell^+\nu_\ell$ decays (in units of 10^{-3}) are given in Tab. II. The experimental results are taken from BESIII measurements [37,38]. For each decay channel, three sets of theoretical predictions are given, corresponding to the form factors from Ref. [30,33] and Ref. [34], respectively. A few remarks are given in order.

- (i) Through this table, one can see that the theoretical results show dramatic dependence on the form factors.
- (ii) Results obtained with the light-front quark model form factors are larger than the data by BESIII experiment, while using the QCD sum rule results, the branching fractions are more consistent with the data.
- (iii) It should be noted again that to accommodate the other data such as $B \rightarrow K_1\gamma$, the mixing angle θ_K is obtained in correlation with the form factors. In Refs. [30,33] this angle is preferred as $\theta_K \sim 45^\circ$, while for Ref. [34], the preferred region is $-47^\circ < \theta_K < -21^\circ$. Thus to estimate the uncertainties from the mixing angle, we have used the consistent value for θ_K with the form factors. We have also checked that if one uses the form factors from Ref. [34] and $30^\circ < \theta_K < 60^\circ$, the resulting branching fraction for $D^0 \rightarrow K^-(1270)e + \nu_e$ is about $(0.21_{-0.14}^{+0.18}) \times 10^{-3}$, which is much smaller than the data. From this table, we can see that the uncertainties are less significant compared to the ones from form factors.

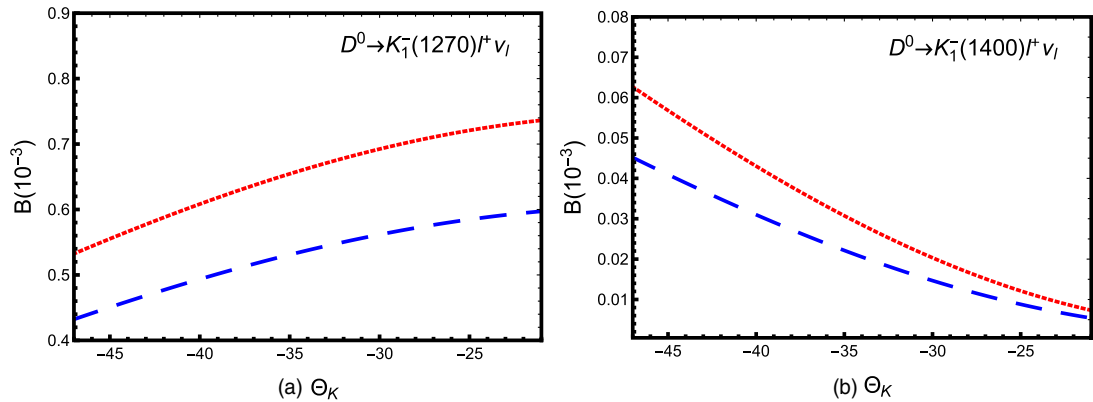


FIG. 6. Dependence of branching ratios $\mathcal{B}(D^0 \rightarrow K_1^- \ell^+ \nu_\ell)$ (in units of 10^{-3}) on the mixing angle Θ_K in the range $-47^\circ < \Theta_K < -21^\circ$ based on the form factors from QCD sum rules [34]. Dotted and dashed curves correspond to the electron and muon mode, respectively.

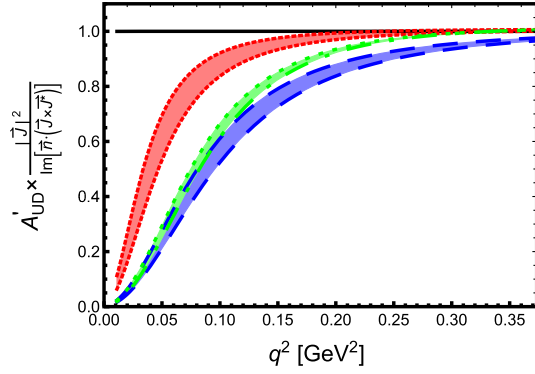


FIG. 7. Results for up-down asymmetry A'_{UD} (in unit of H_{K_1}) in $D \rightarrow K_1(\rightarrow K\pi\pi)\ell^+\nu_\ell$. The solid curve corresponds to the electron final state, in which the lepton mass is negligible and the result is very close to unity. The results shadowed in red (upper) and blue (lower) correspond to the muon mode with form factors from light-front quark model in Ref. [30,33], respectively, while the green band (middle) is obtained using the QCD sum rules in Ref. [34], respectively. The nonzero mass of μ provides sizable corrections as shown in Eq. (29).

Figure 5 and Fig. 6 show the dependence of branching fractions $\mathcal{B}(D^0 \rightarrow K_1^-\ell^+\nu_\ell)$ (in units of 10^{-3}) on the mixing angle Θ_K . Dotted and dashed curves correspond to the electron and muon mode, respectively.

C. Angular distributions

Results for up-down asymmetry A'_{UD} (in unit of H_{K_1}) in $D \rightarrow K_1\ell^+\nu_\ell$ are shown in Fig. 7. The solid curve corresponds to the electron final state, in which the lepton mass is negligible and the result is very close to unity. The results shadowed in red (upper) and blue (lower) correspond to the muon mode with form factors from light-front quark model in Ref. [30,33], respectively, while the green band (middle) is obtained using the QCD sum rules in Ref. [34], respectively. From this figure, one can see that the nonzero mass of muon can give considerable corrections also shown in Eq. (29). The results on the asymmetry are also dependent on the dynamical form factors, which can be tested in experiment.

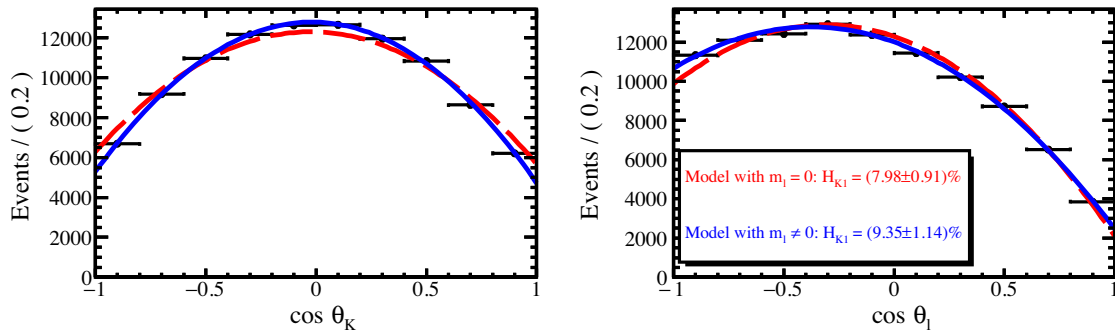


FIG. 8. Fit to 1.0×10^5 MC events with 3 components using two models: $m_l = 0$ (Red) and $m_l \neq 0$ (Blue)

Integrating over the q^2 , we obtain the angular distributions of $D \rightarrow K_1(\rightarrow K\pi\pi)\ell^+\nu_\ell$ dataset as

$$\begin{aligned} \frac{d\Gamma}{d\cos\theta_\ell d\cos\theta_K} = & a_1 + a_2[\cos^2\theta_K \cos^2\theta_\ell] + a_3 \cos\theta_\ell \\ & + a_4 \cos^2\theta_K \cos\theta_\ell + a_5 \cos\theta_K \\ & + a_6 \cos\theta_K \cos^2\theta_\ell + a_7 \cos\theta_K \cos\theta_\ell \\ & + a_8 \cos^2\theta_K + a_9 \cos^2\theta_\ell, \end{aligned} \quad (45)$$

with

$$a_i = \frac{3}{8} \int dq^2 \frac{G_F^2 V_{cs}^2 q^2 \sqrt{\lambda(m_D^2, m_{K_1}^2, q^2)}}{512\pi^3 m_D^3} (1 - m_\ell^2/q^2)^2 \times d_i. \quad (46)$$

As an illustration, we use a standalone fast simulation software RapidSim [39] with the LHCb geometrical acceptance to generate MC samples. The $D^0 \rightarrow K_1(1270)^-\mu^+\nu_\mu$ decays are described by EVTGEN [40], and the $K_1(1270)^-$ meson is allowed to decay into all intermediate processes that result in a $K^-\pi^+\pi^-$ final state. The BFs of $K_1(1270)^-$ meson subdecays measured by Belle [41] are used as inputs in the simulation. Based on 2 fb^{-1} data recorded at 8 TeV, LHCb observed close to 2000 $D^{*+} \rightarrow D^0\pi^+$, $D^0 \rightarrow K^-\pi^+\mu^+\mu^-$ signal candidates in the ρ/ω mass region [42]. As $\mathcal{B}(D^0 \rightarrow K_1(1270)^-(\rightarrow K^-\pi^+\pi^-)\mu^+\nu_\mu)$ is expected to be about two orders of magnitude higher than the known $\mathcal{B}(D^0 \rightarrow K^-\pi^+[\mu^+\mu^-]_{\rho/\omega})$ [27], it is reasonable to estimate that $\mathcal{O}(10^5)$ $D^{*+} \rightarrow D^0\pi^+$, $D^0 \rightarrow K_1(1270)^-\mu^+\nu_\mu$ signal candidates can be collected based on 9 fb^{-1} Runs 1–2 data from LHCb. Therefore, to have a rough estimation on the LHCb sensitivity, we have generated about 1.0×10^5 $D^{*+} \rightarrow D^0\pi^+$, $D^0 \rightarrow K_1(1270)^-(\rightarrow K^-\pi^+\pi^-)\mu^+\nu_\mu$ events without considering any detector resolution effects.

A comparison of fitting these MC samples using the formula (45) and the one from previous work [24] is given in Fig. 8. Through these figures, one can see that our simulated angular distributions can not be well described

by the angular distribution in the previous work [24]. With the inclusion of the muon mass, the agreement between theoretical description and angular distributions of MC events is greatly improved, and the fitted H_{K_1} is compatible with the input of 9.2% based on the SM expectation [24]. The statistical uncertainty for H_{K_1} is 1.1%.

IV. SUMMARY

Weak decays of heavy quarks have played an important role in testing standard model and probing new physics beyond. Recent studies of flavor-changing neutral current process has revealed some hints for potential NP effects (see for instance Ref. [43]), but a conclusive result is far from well-established, and requests more dedicated theoretical and experimental studies in future [44]. At the same time, the photon helicity in $b \rightarrow s\gamma$ might render very competitive potentials for new physics.

Compared to the previous WYZ method [24] in which a ratio of up-down asymmetries in $D \rightarrow K_1(\rightarrow K\pi\pi)e^+\nu_e$, \mathcal{A}'_{UD} , has been proposed to quantify the hadronic effects in $K_1 \rightarrow K\pi\pi$ decay, we have in this work systematically derived differential decay widths and angular distributions for the decay cascade $D \rightarrow K_1(1270, 1400)\ell^+\nu_\ell \rightarrow (K\pi\pi)\ell^+\nu_\ell$ ($\ell = e, \mu$). In the derivation, the mass of electron/muon is explicitly included. Using the $D \rightarrow K_1$ form factors from light-front quark model and QCD sum rule, we have calculated partial decay widths and branching fractions for $D^0 \rightarrow K_1^-\ell^+\nu_\ell$ and $D^+ \rightarrow K_1^0\ell^+\nu_\ell$, but

pointed out that these theoretical results for $\mathcal{B}(D \rightarrow K_1e^+\nu_e)$ show dramatic dependence on the form factors.

With the angular coefficients, we have demonstrated that the measurement of up-down asymmetry in $D \rightarrow K_1e^+\nu_e \rightarrow (K\pi\pi)e^+\nu_e$ and the angular distribution in $D \rightarrow K_1\ell^+\nu_\ell \rightarrow (K\pi\pi)\ell^+\nu_\ell$ can help to pin down hadronic uncertainties in $B \rightarrow K_1(\rightarrow K\pi\pi)\gamma$. Based on Monte-Carlo simulation, we have found that after including the muon mass, the angular distributions can be well described by the theoretical framework. Performing an angular analysis using Eq. (45) on a sample of $10^5 D^0 \rightarrow K_1(1270)^-(\rightarrow K^-\pi^+\pi^-)\mu^+\nu_\mu$ decays corresponding to the signal statistics assumed for LHCb in Runs 1–2 leads to a statistical uncertainty of $\sim 1.1\%$ on H_{K_1} .

ACKNOWLEDGMENTS

W. W. thanks Fu-Sheng Yu and Zhen-Xing Zhao for valuable discussions and the collaboration at the early stage of this work. The authors are grateful to Fei Huang, Xian-Wei Kang, Xiao-Rui Lyu, Wen-Bin Qian, Yang-Heng Zheng for useful discussions. This work is supported in part by National Natural Science Foundation of China under Grants No. 11735010, No. U2032102, No. 12061131006, and No. 12061141006, by Natural Science Foundation of Shanghai under Grant No. 15DZ2272100, by Joint Large-Scale Scientific Facility Funds of the NSFC and CAS under Grant No. U1932108.

-
- [1] D. Atwood, M. Gronau, and A. Soni, *Phys. Rev. Lett.* **79**, 185 (1997).
 - [2] D. Becirevic, E. Kou, A. Le Yaouanc, and A. Tayduganov, *J. High Energy Phys.* **08** (2012) 090.
 - [3] A. Paul and D. M. Straub, *J. High Energy Phys.* **04** (2017) 027.
 - [4] E. Kou, C. D. Lü, and F. S. Yu, *J. High Energy Phys.* **12** (2013) 102.
 - [5] N. Haba, H. Ishida, T. Nakaya, Y. Shimizu, and R. Takahashi, *J. High Energy Phys.* **03** (2015) 160.
 - [6] B. Aubert *et al.* (BABAR Collaboration), *Phys. Rev. D* **77**, 051103 (2008).
 - [7] J. P. Lees *et al.* (BABAR Collaboration), *Phys. Rev. Lett.* **109**, 191801 (2012).
 - [8] J. P. Lees *et al.* (BABAR Collaboration), *Phys. Rev. D* **86**, 052012 (2012).
 - [9] T. Saito *et al.* (Belle Collaboration), *Phys. Rev. D* **91**, 052004 (2015).
 - [10] Y. Ushiroda *et al.* (Belle Collaboration), *Phys. Rev. D* **74**, 111104 (2006).
 - [11] B. Aubert *et al.* (BABAR Collaboration), *Phys. Rev. D* **78**, 071102 (2008).
 - [12] R. Aaij *et al.* (LHCb Collaboration), *Phys. Rev. Lett.* **123**, 081802 (2019).
 - [13] S. Akar, E. Ben-Haim, J. Hebing, E. Kou, and F. S. Yu, *J. High Energy Phys.* **09** (2019) 034.
 - [14] Y. Grossman and D. Pirjol, *J. High Energy Phys.* **06** (2000) 029.
 - [15] R. Aaij *et al.* (LHCb Collaboration), *J. High Energy Phys.* **12** (2020) 081.
 - [16] S. de Boer and G. Hiller, *Eur. Phys. J. C* **78**, 188 (2018).
 - [17] N. Adolph, G. Hiller, and A. Tayduganov, *Phys. Rev. D* **99**, 075023 (2019).
 - [18] M. Gronau, Y. Grossman, D. Pirjol, and A. Ryd, *Phys. Rev. Lett.* **88**, 051802 (2002).
 - [19] M. Gronau and D. Pirjol, *Phys. Rev. D* **66**, 054008 (2002).
 - [20] E. Kou, A. Le Yaouanc, and A. Tayduganov, *Phys. Rev. D* **83**, 094007 (2011).
 - [21] R. Aaij *et al.* (LHCb Collaboration), *Phys. Rev. Lett.* **112**, 161801 (2014).
 - [22] A. Tayduganov, E. Kou, and A. Le Yaouanc, *Phys. Rev. D* **85**, 074011 (2012).
 - [23] M. Gronau and D. Pirjol, *Phys. Rev. D* **96**, 013002 (2017).

- [24] W. Wang, F. S. Yu, and Z. X. Zhao, *Phys. Rev. Lett.* **125**, 051802 (2020).
- [25] R. H. Li, C. D. Lu, and W. Wang, *Phys. Rev. D* **79**, 034014 (2009).
- [26] W. Wang and Z. X. Zhao, *Eur. Phys. J. C* **76**, 59 (2016).
- [27] P. A. Zyla *et al.* (Particle Data Group), *Prog. Theor. Exp. Phys.* **2020**, 083C01 (2020).
- [28] K. C. Yang, *Nucl. Phys.* **B776**, 187 (2007).
- [29] K. Abe *et al.* (Belle Collaboration), [arXiv:hep-ex/0408138](https://arxiv.org/abs/hep-ex/0408138).
- [30] R. C. Verma, *J. Phys. G* **39**, 025005 (2012).
- [31] H. Y. Cheng and X. W. Kang, *Eur. Phys. J. C* **77**, 587 (2017); *Eur. Phys. J. C* **77**, 863(E) (2017).
- [32] Q. Chang, X. L. Wang, and L. T. Wang, *Chin. Phys. C* **44**, 083105 (2020).
- [33] H. Y. Cheng, C. K. Chua, and C. W. Hwang, *Phys. Rev. D* **69**, 074025 (2004).
- [34] S. Momeni and R. Khosravi, *J. Phys. G* **46**, 105006 (2019).
- [35] R. Khosravi, K. Azizi, and N. Ghahramany, *Phys. Rev. D* **79**, 036004 (2009).
- [36] S. Momeni, *Eur. Phys. J. C* **80**, 553 (2020).
- [37] M. Ablikim *et al.* (BESIII Collaboration), *Phys. Rev. Lett.* **123**, 231801 (2019).
- [38] M. Ablikim *et al.* (BESIII Collaboration), [arXiv:2102.10850](https://arxiv.org/abs/2102.10850).
- [39] G. A. Cowan, D. C. Craik, and M. D. Needham, *Comput. Phys. Commun.* **214**, 239 (2017).
- [40] D. J. Lange, *Nucl. Instrum. Methods Phys. Res., Sect. A* **462**, 152 (2001).
- [41] H. Guler *et al.* (Belle Collaboration), *Phys. Rev. D* **83**, 032005 (2011).
- [42] R. Aaij *et al.* (LHCb Collaboration), *Phys. Rev. Lett.* **119**, 181805 (2017).
- [43] R. Aaij *et al.* (LHCb Collaboration), [arXiv:2103.11769](https://arxiv.org/abs/2103.11769).
- [44] A. Cerri, V. V. Gligorov, S. Malvezzi, J. M. Camalich, J. Zupan, S. Akar, J. Alimena, B. C. Allanach, W. Altmannshofer, L. Anderlini *et al.*, CERN Yellow Rep. Monogr. **7**, 867 (2019).